

Examination of Cerebral Aneurysm by Scanning Acoustic Microscopy

Bukem Tanoren (✉ bukem.bilen1@boun.edu.tr)

Bogazici University

Research article

Keywords: Scanning acoustic microscopy, cerebral aneurysm, acoustic impedance, subarachnoid hemorrhage

Posted Date: August 13th, 2020

DOI: <https://doi.org/10.21203/rs.3.rs-42814/v1>

License:  This work is licensed under a Creative Commons Attribution 4.0 International License.

[Read Full License](#)

1 Examination of Cerebral Aneurysm

2 by Scanning Acoustic Microscopy

3 Bukem Tanoren

4 Bogazici University, Department of Physics, Istanbul, Turkey

5 bukem.bilen1@boun.edu.tr

6 ORCID: 0000-0001-7992-0501

7

8 Abstract

9 **Background:** Asymptomatic intracranial aneurysms rupture without any
10 warning, therefore, use of high-resolution imaging techniques for the rupture risk
11 assessment is essential.

12 **Methods:** This study's goal is to assess the feasibility of scanning acoustic
13 microscopy (SAM) in the characterization of cerebral aneurysm. The aneurysm's
14 dome samples were obtained from 12 different patients with and without
15 subarachnoid hemorrhage.

16 **Results:** The acoustic impedance values are found statistically higher in samples
17 from female patients than in samples from male patients. On the other hand,
18 sample from a male patient without subarachnoid hemorrhage has higher acoustic
19 impedance value when compared with samples from male patients with
20 subarachnoid hemorrhage, however, this discrepancy is not observed in female
21 patients.

22 **Conclusion:** In summary, the success of SAM in monitoring the altering acoustic
23 impedance values in male and female patients with and without subarachnoid
24 hemorrhage indicates the potential of SAM for the diagnosis of instability of
25 cerebral aneurysms.

26

27 **Keywords**

28 Scanning acoustic microscopy, cerebral aneurysm, acoustic impedance,
29 subarachnoid hemorrhage

30 **Abbreviations**

Scanning acoustic microscopy	SAM
Brain magnetic resonance imaging	MRI
Computed tomography angiography	CTA
Digital subtraction angiography	DSA
Magnetic resonance angiography	MRA
Optical coherence tomography	OCT
Acoustic impedance	AI

31

32 **Declarations**

33 **Funding** This study was funded by the Ministry of Development of Turkey (grant
34 number 2009K120520).

35 **Conflicts of interest/Competing interests** The author declares that she has no
36 conflict of interest.

37 **Ethics approval** All procedures performed in studies involving human
38 participants were in accordance with the ethical standards of the institutional
39 and/or national research committee and with the 1964 Helsinki and its later
40 amendments or comparable ethical standards. The study was approved by the
41 Ethics Committee of Biruni University.

42 **Consent to participate** Written informed consent was obtained from all
43 individual participants included in the study.

44 **Consent for publication** Informed consent was obtained from all individual
45 participants included in the study.

46 **Availability of data and material** The datasets used and/or analyzed during the
47 current study are available from the corresponding author on reasonable request.

48 **Code availability** Not applicable.

49 **Acknowledgments**

50 I want to thank to Assoc. Prof. Kamran Aghayev from Biruni University,
51 Istanbul, Turkey for providing the tissues studied in this study and the Ministry of
52 Development of Turkey (grant number 2009K120520) for supporting scanning
53 acoustic microscopy. I also want to thank to Prof. Mehmet Burcin Unlu from
54 Bogazici University, Istanbul, Turkey for letting me use all of the facilities in his
55 laboratory.

56

57 **Introduction**

58

59 Dilations of blood vessels within the brain are called cerebral aneurysms. At major
60 branch points in the Circle of Willis [1], weakening of media wall cause cerebral
61 aneurysms and their rupture causes subarachnoid hemorrhage [2] associated with
62 high mortality rates, therefore, diagnosis and definitive treatment of cerebral
63 aneurysms, before or very shortly after rupture, are crucial. Treatment is done
64 either with clipping or coiling [3] and aneurysm exclusion is evaluated with
65 angiography, which includes contrast agent injection and can only reveal vessel
66 shape. On the other hand, healing of treated aneurysms has to be followed and
67 currently, there are no modalities available in clinics for visualization of healing
68 process with sufficient resolution. These disabilities urge many researchers to
69 develop new imaging techniques.

70

71 Brain magnetic resonance imaging (MRI) is a frequently used in the diagnosis of
72 intracranial hemorrhage. Monitoring methods such as computed tomography
73 angiography (CTA), digital subtraction angiography (DSA) and magnetic
74 resonance angiography (MRA) are used in cranial vascular pathologies [4, 5].
75 Even though, these angiographic methods provide high accuracy results, they

76 have advantages and disadvantages over each other. MRA uses intravenous
77 contrast agents and repeated ionizing radiation exposure for producing a high-
78 resolution image. The gold standard method for the detection of intracranial
79 aneurysms is DSA but it is an expensive modality. On the other hand, CTA is
80 cheaper and also non-invasive when compared to DSA. Optical coherence
81 tomography (OCT) endovascular catheter reveals the vessel wall structure with a
82 high resolution, providing information for the assessment of the vessel healing
83 progress [6], however, flushing of blood is necessary for a good OCT signal.
84 Scanning acoustic microscopy (SAM) will be an alternative to these investigation
85 tools. SAM can supply morphological and mechanical information
86 simultaneously, with micro-meter level resolution. Ultrasound signals are used to
87 define the elastic properties of biological tissues by calculating sound speed
88 through tissues [7-9] or acoustic impedance of the tissues [10]. When compared
89 with the techniques previously mentioned, SAM has the advantage of micro-meter
90 level resolution, the capability of non-destructive monitoring, no requirement of
91 a special sampling, the ability of quick measurement (less than 2 minutes for a 4.8
92 mm x 4.8 mm area) [11] and the applicability to tissues [12-15] or cell populations
93 [16-20]. Besides, a SAM probe would enable its use in clinics [21].

94

95 Here, we reported the first application of SAM system, equipped with an 80 MHz
96 transducer, offering a lateral resolution of approximately 20 μm , for the
97 characterization of cerebral aneurysm's dome samples. For this purpose, acoustic
98 impedance mode of SAM was used and the acoustic impedance values of the
99 specimen were recorded. The findings indicate that SAM can resolve variations
100 in samples of male and female with and without subarachnoid hemorrhage,
101 therefore, for the quantitative assessment of life-threatening aneurysms in clinics
102 SAM is a promising tool, offering benefits of micro-meter level resolution by

103 preserving sample's integrity, non-destructive and easy-to-perform mechanism
104 and rapid measurement.

105 **Materials and Methods**

106

107 **Specimens**

108

109 This study was ethically approved by Biruni University Ethics Committee and
110 informed consent was obtained from each participant. Aneurysm's dome samples
111 were obtained after microsurgical clipping. Briefly, standard pterional craniotomy
112 was performed and the aneurysm was exposed by opening the Sylvian fissure and
113 gradually dissecting the originating vessel. After establishing proximal and distal
114 control, the aneurysm's neck was dissected and a permanent clip was placed.
115 Following the clip ligation, the aneurysm's dome was dissected from surrounding
116 tissue and cut as close to the clip as possible. Immediately after removal, the dome
117 was preserved in 4 % formaldehyde solution for SAM studies.

118

119 **Scanning Acoustic Microscopy**

120

121 The methods were carried out in accordance with Bogazici University
122 Institutional Review Board for Research with Human Subjects. The aneurysm's
123 dome tissues were examined by scanning acoustic microscope (AMS-50SI) built
124 by Honda Electronics (Toyohashi, Japan). Fig. 1 shows acoustic impedance (AI)
125 mode schematic of SAM setup. A transducer with a quartz lens, a pulser/receiver,
126 an oscilloscope, a computer with a display monitor constitute SAM setup. The
127 spot size of 80 MHz transducer is 17 μm and its focal length is 1.5 mm. It is a
128 pulser/receiver, since it collects the reflected acoustic waves as well as sending
129 them. Distilled water is the coupler the quartz lens and the substrate. For two-
130 dimensional scanning of the transducer, there is an X-Y stage. The signals,

131 reflected from the reference and also the target material, are analyzed by the
132 oscilloscope. Finally, the maps of acoustic intensity and impedance with a lateral
133 resolution of approximately 20 μm are visualized with 300 x 300 sampling points.

134

135 The signal reflected from the target material in Fig. 1 is

136

$$S_{target} = \frac{Z_{target}-Z_{sub}}{Z_{target}+Z_{sub}} S_0 \quad (1)$$

137 where, S_0 is the signal transducer generates, Z_{target} is target material's acoustic
138 impedance and Z_{sub} is the polystyrene substrate's acoustic impedance (2.37
139 MRayl). The signal reflected from the reference is

140

141

$$S_{ref} = \frac{Z_{ref}-Z_{sub}}{Z_{ref}+Z_{sub}} S_0 \quad (2)$$

142

143 where, Z_{ref} is the acoustic impedance of distilled water (1.50 MRayl). Then,
144 acoustic impedance of the target under investigation is given as

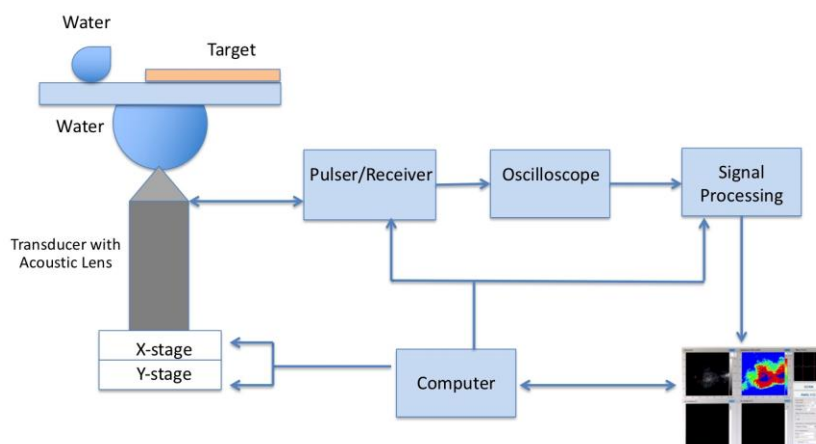
145

$$Z_{target} = \frac{\frac{S_{target}}{S_0}}{\frac{S_{target}}{S_0}} Z_{sub} \quad (3)$$

146

147 with a constant signal S_0 [19], transducer generates.

148



149

150

151 **Fig. 1.** AI mode schematic of SAM. The signals reflected from water and the
152 aneurysm's dome sample surfaces are combined for the acoustic impedance value
153 calculation of the tissue.

154

155 **Results**

156

157 Aneurysm's dome samples received from patients were very thin, therefore like
158 two-dimensional structures with plain facets, and were examined by using AI
159 mode. Fig. 2 shows the acoustic impedance map of a male aneurysm's dome
160 sample. This map was constructed by collecting the ultrasound signals reflected
161 from reference (water) surface and the aneurysm's dome sample surface on the
162 polystyrene substrate. As can be seen in Fig. 2, acoustic impedance is smaller than
163 2 MRayl. Table 1 presents average acoustic impedance values of all dome samples
164 studied in this investigation.

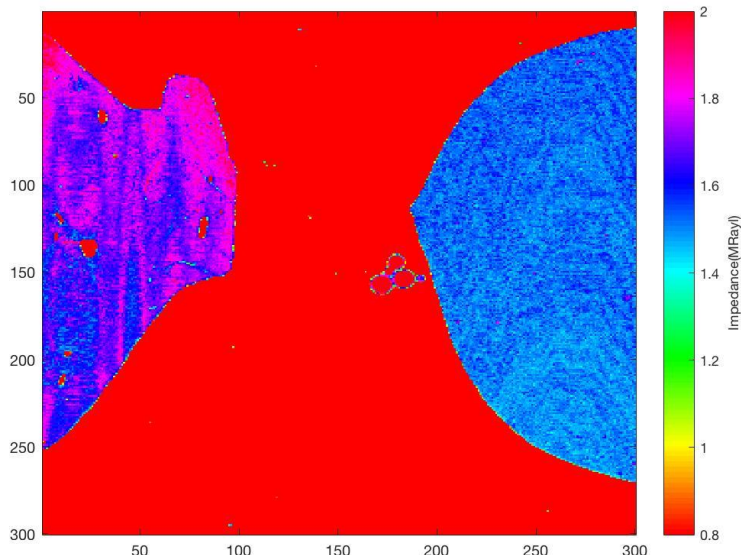
165

166 **Table 1.** Average acoustic impedance values of aneurysm's dome samples of
167 male and female patients with and without subarachnoid hemorrhage. 6 female
168 and 6 male patients were studied for the correlation of gender and hemorrhage on
169 the dome sample.

Gender	Acoustic Impedance (MRayl)	Hemorrhage
Male	1.853 ± 0.061	Yes
Male	1.821 ± 0.049	Yes
Male	1.850 ± 0.083	Yes
Male	1.890 ± 0.022	Yes
Male	1.893 ± 0.039	Yes
Male	2.007 ± 0.031	No

Female	1.943 ± 0.032	Yes
Female	2.093 ± 0.018	Yes
Female	2.030 ± 0.031	Yes
Female	2.068 ± 0.019	Yes
Female	2.041 ± 0.024	Yes
Female	2.027 ± 0.024	No

170



171

172 **Fig. 2.** Acoustic impedance map of a male aneurysm's dome sample, obtained by
 173 comparing the reflected ultrasound signals from the surfaces of water and the
 174 dome sample, with 300×300 sampling points, in a scanning area of $4.8 \text{ mm} \times 4.8$
 175 mm. Distilled water droplet, which has the acoustic impedance of 1.5 MRayl, is
 176 more homogeneous shape on the right.

177

178 Discussion

179

180 We have shown that SAM can characterize aneurysm's dome samples by the
 181 calculation of the acoustic impedance. The acoustic impedance values are

182 calculated to be higher for all female patients' samples with and without
183 subarachnoid hemorrhage when compared to male patients' samples with
184 subarachnoid hemorrhage, indicating gender dependence on the contents of
185 aneurysm's dome samples. Age interval of the patients is chosen quite narrow,
186 between 50 and 60, and almost all of the patients have hemorrhage, only 1 male
187 and 1 female have no subarachnoid hemorrhage. We assume that these
188 observations are due to parameters like gender or lifestyles, which influence
189 aneurysm development. The higher acoustic impedance value is observed a result
190 of higher elastic modulus. Aneurysm dome samples of female patients with and
191 without subarachnoid hemorrhage are firmer and therefore easily distinguishable.
192 On the other hand, there is no significant discrepancy in acoustic impedance
193 values of dome samples of female patients with and without subarachnoid
194 hemorrhage, which is an indication of no hemorrhage dependence in female
195 patients. In male patients' samples, hemorrhage has an effect on acoustic
196 impedance, in other words, on elasticity, therefore, samples with hemorrhage,
197 which are softer tissues, have lower acoustic impedance values.

198

199 All of aneurysm's dome samples, received from female and male patients, were
200 firmer than normal vessel tissue, however, in this study, we only studied samples
201 with or without hemorrhage but not a normal vessel tissue sample, therefore, we
202 were unable to compare our results with a reference. 6 male and 6 female patients
203 with and without subarachnoid hemorrhage were studied for the correlation of
204 gender and hemorrhage on dome samples. Two-dimensional maps, as in Fig. 2,
205 are acquired with micro-meter level resolution and average acoustic impedances
206 are calculated. As can be seen in Table 1, dome sample of male patient without a
207 subarachnoid hemorrhage, has the highest acoustic impedance value, when
208 compared with those of other male patients. In other words, almost all patients
209 had hemorrhage which are detected due to symptoms like severe headache or

210 nausea, patients have just after hemorrhage starts. Brain aneurysms below 4 mm
211 are not detectable with conventional imaging methods and when aneurysm is
212 more than 7 mm [22], it is more likely to rupture causing subarachnoid
213 hemorrhage, which may take place at any time. Ruptured aneurysms are closely
214 related to mortality and morbidity. Therefore, discrimination of dome samples of
215 male patients with and without subarachnoid hemorrhage by SAM is an indicator
216 of the feasibility of this modality in the diagnosis of aneurysms prone to rupture
217 in clinics.

218

219 Conclusion

220

221 Here, we present the capability of SAM in characterizing the cerebral aneurysm's
222 dome samples for the first time. Acoustic impedance maps of the tissues display
223 distinctive values in male and female patients. On the other hand, hemorrhage
224 has an apparent effect on samples of male patients, while there is no significant
225 difference in female patients' samples. Consequently, we can say that SAM has a
226 potential as an imaging tool in clinics and will be able to do rupture risk
227 assessment, since it can acquire information about the morphology and elasticity
228 of the samples. However, first, SAM has to be developed on a probe for direct
229 evaluation of vessel wall structure during surgeries.

230

231 References

- 232 1- Cebral JR, Raschi M (2013) Suggested connections between risk
233 factors of intracranial aneurysms: a review. Ann Biomed Eng 41:1366–
234 1383
- 235 2- Van Gijn J, Rinkel GJE (2001) Subarachnoid hemorrhage: diagnosis,
236 causes and management. Brain 124:249–278
- 237 3- Ruan C, Long H, Sun H, He M, Yang K, Zhang H, Mao B (2015)

- 238 Endovascular coiling vs. surgical clipping for unruptured intracranial
239 aneurysm. A meta-analysis. *Brit J Neurosurg* 29(4):485–492
- 240 4- Delgado Almandoz JE, Jagadeesan BD, Refai D, Moran CJ, Cross
241 DT3rd, Chicoine MR, Rich KM, Diringer MN, Dacey RGJr, Derdeyn
242 CP, Zipfel GJ (2012) Diagnostic yield of computed tomography
243 angiography and magnetic resonance angiography in patients with
244 catheter angiography- negative subarachnoid hemorrhage. *J Neurosurg*
245 117:309- 315
- 246 5- Prestigiacomo CJ, Sabit A, He W, Jethwa P, Gandhi C, Russin J (2010)
247 Three dimensional CT angiography versus digital subtraction
248 angiography in the detection of intracranial aneurysms in subarachnoid
249 hemorrhage. *J Neurointerv Surg* 2:385- 389
- 250 6- Jianping S, Marlon SM, Chiedozie I, Nwagwu AE, Binh VN, Mehrzad
251 H, Mark EL, Zhongping C (2008) Imaging Treated Brain Aneurysms in
252 vivo using Optical Coherence Tomography. *Proc of SPIE* 6847: 684732-
253 1
- 254 7- Saijo Y, Filho ES, Sasaki H, Yambe T, Tanaka M, Hozumi N, Kobayashi
255 K, Okada N (2007) Ultrasonic tissue characterization of atherosclerosis
256 by a speed-of-sound microscanning system. *IEEE Trans Ultrason
257 Ferroelectr Freq Control* 54 (8):1571-1577
- 258 8- Brewin MP, Srodon PD, Greenwald SE, Birch MJ (2014) Carotid
259 atherosclerotic plaque characterization by measurement of ultrasound
260 sound speed in vitro at high frequency, 20 MHz. *Ultrasonics* 54:428-441
- 261 9- Saijo Y, Miyakawa T, Sasaki H, Tanaka M, Nitta S (2004) Acoustic
262 properties of aortic aneurysm obtained with scanning acoustic
263 microscopy. *Ultrasonics* 42:695-698
- 264 10- Kobayashi K, Yoshida S, Saijo Y, Hozumi N (2014) Acoustic impedance
265 microscopy for biological tissue characterization. *Ultrasonics* 54:1922-

- 266 1928
- 267 11- Briggs A (1985) An introduction to scanning acoustic microscopy.
- 268 Oxford University Press, Oxford
- 269 12- Raum K, Kempf K, Hein HJ, Schubert J, Maurer P (2007) Preservation
- 270 of microelastic properties of dentin and tooth enamel *in vivo* - a
- 271 scanning acoustic microscopy study. Dental Materials 23(10):1221-
- 272 1228
- 273 13- Irie S, Inoue K, Yoshida K, Mamou J, Kobayashi K, Maruyama H,
- 274 Yamaguchi T (2016) Speed of sound in diseased liver observed by
- 275 scanning acoustic microscopy with 80 MHz and 250 MHz. J Acoust
- 276 Soc Am 139:512-519
- 277 14- Ito K, Yoshida K, Maruyama H, Mamou J, Yamaguchi T (2017)
- 278 Acoustic Impedance Analysis with High-Frequency Ultrasound for
- 279 Identification of Fatty Acid Species in the Liver. Ultrasound Med Biol
- 280 43:700-711
- 281 15- Saijo Y, Tanaka M, Okawai H, Dunn F (1991) The ultrasonic
- 282 properties of gastric cancer tissues obtained with a scanning acoustic
- 283 microscope system. Ultrasound Med Biol 17:709-714
- 284 16- Kundu T, Bereiter-Hahn J, Karl I (2000) Cell property determination
- 285 from the acoustic microscope generated voltage versus frequency
- 286 curves. Biophys J 78:2270-2279
- 287 17- Zhao X, Akhtar R, Nijenhuis N, Wilkinson SJ, Murphy L, Ballestrem
- 288 C, Derby B (2012) Multi-layer phase analysis: quantifying the elastic
- 289 properties of soft tissues and live cells with ultra-high-frequency
- 290 scanning acoustic microscopy. IEEE Trans Ultrason Ferroelectr Freq
- 291 Control 59:610-620

- 292 18- Miura K, Nasu H, Yamamoto S (2013) Scanning acoustic microscopy
293 for characterization of neoplastic and inflammatory lesions of lymph
294 nodes. *Sci Rep* 3:1255
- 295 19- Miura K, Yamamoto S (2015) A scanning acoustic microscope
296 discriminates cancer cells in fluid. *Sci Rep* 5:15243
- 297 20- Soon TTK, Chean TW, Yamada H, Takahashi K, Hozumi N,
298 Kobayashi K, Yoshida S (2017) Effects of anticancer drugs on glia-
299 glioma brain tumor model characterized by acoustic impedance
300 microscopy. *Jpn J Appl Phys* 56(7S1):07JF15
- 301 21- Hatori K, Saijo Y, Hagiwara Y, Naganuma Y, Igari K, Iikubo M,
302 Kobayashi K, Sasaki K (2016) Acoustic diagnosis device for dentistry.
303 In: Sasaki K, Suzuki O, Takahashi N (eds.) *Interface Oral Health*
304 *Science*, Springer, Singapore, pp. 181-201
- 305 22- Villablanca JP, Duckwiler GR, Jahan R, Tateshima S, Martin NA,
306 Frazee J, Gonzales NR, Sayre J, Vinuela FV (2013) Natural history of
307 asymptomatic unruptured cerebral aneurysms evaluated at CT
308 angiography: Growth and rupture incidence and correlation with
309 epidemiologic risk factors. *Radiology* 269:258- 65

Figures

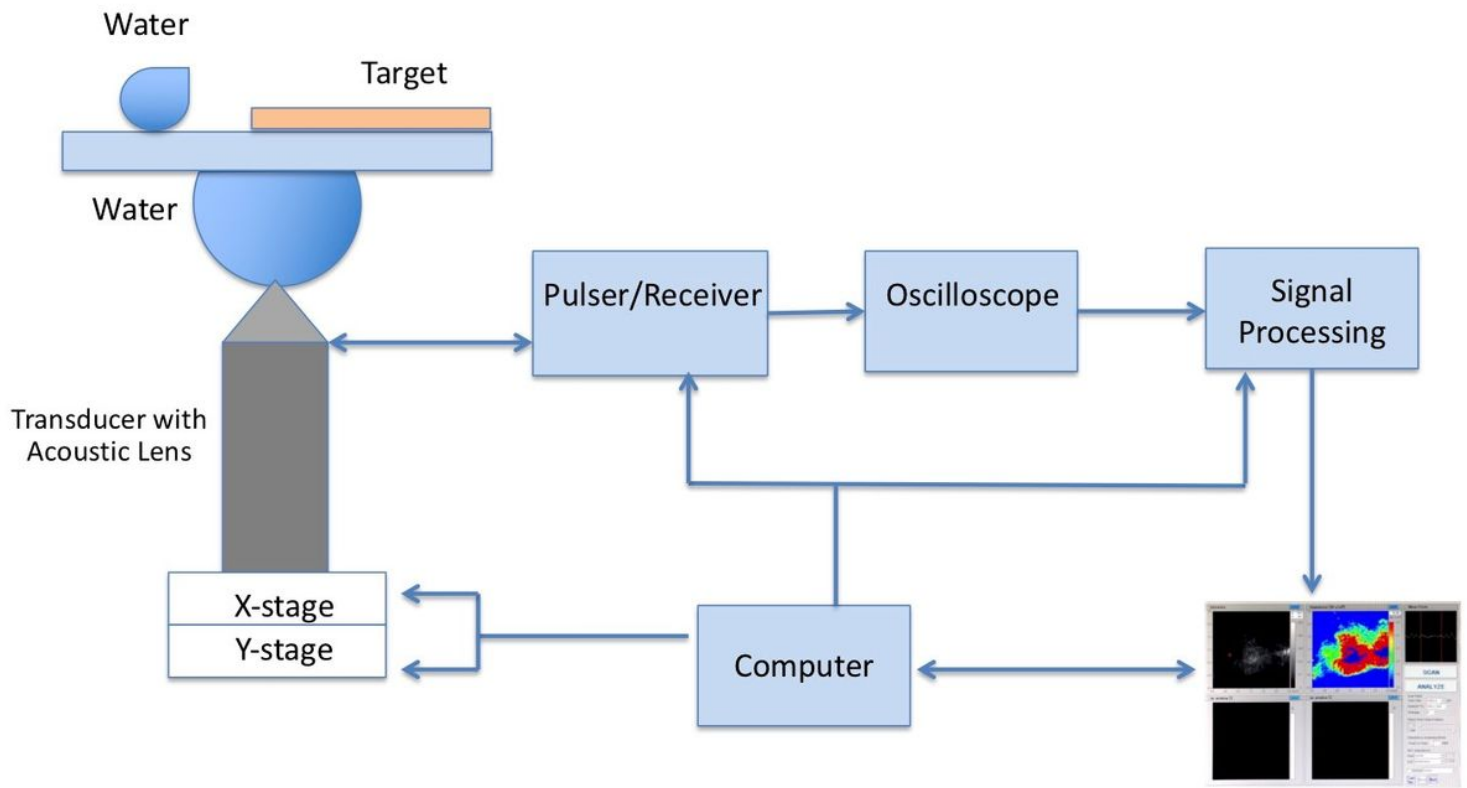


Figure 1

AI mode schematic of SAM. The signals reflected from water and the aneurysm's dome sample surfaces are combined for the acoustic impedance value calculation of the tissue.

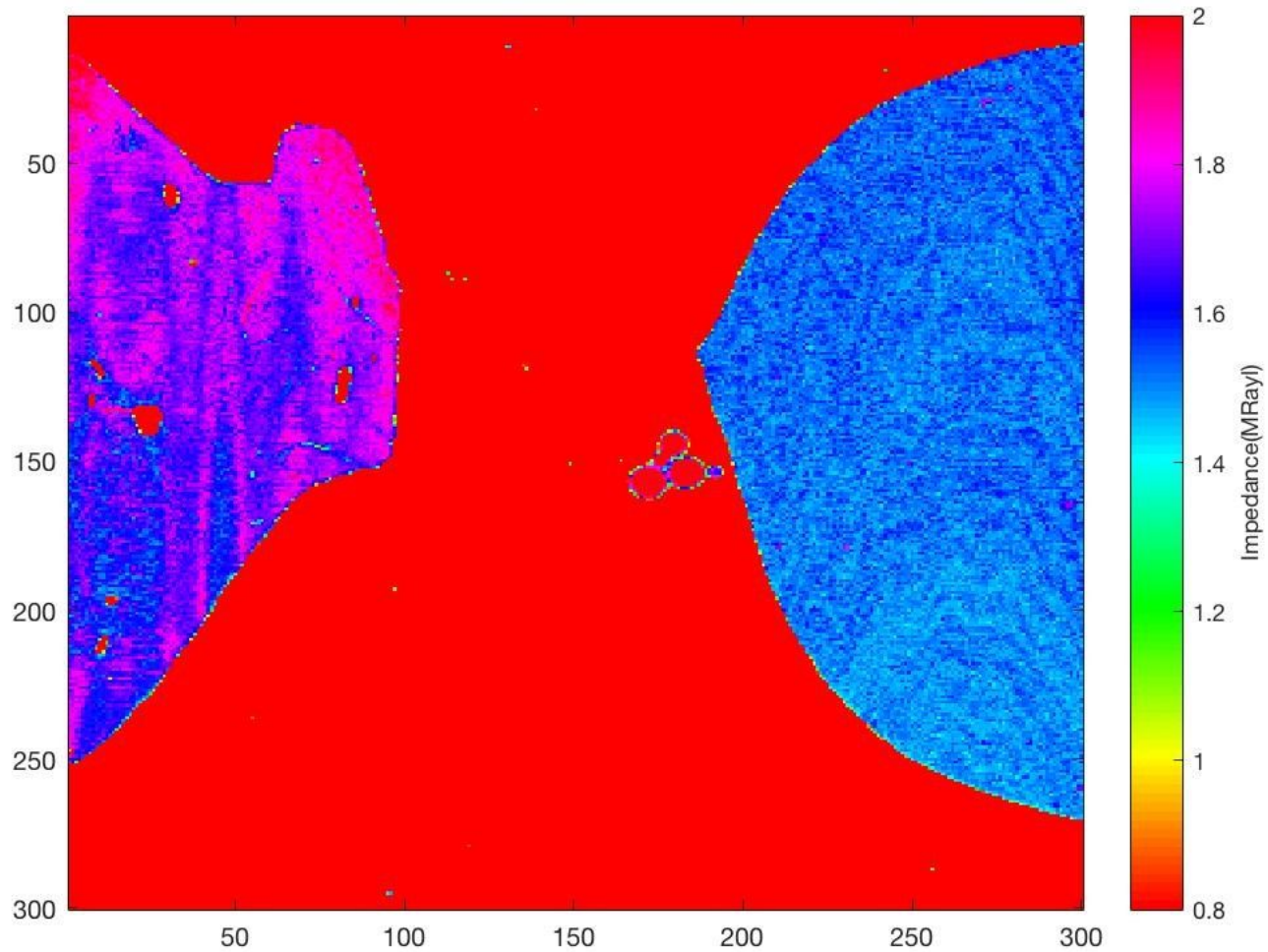


Figure 2

Acoustic impedance map of a male aneurysm's dome sample, obtained by comparing the reflected ultrasound signals from the surfaces of water and the dome sample, with 300×300 sampling points, in a scanning area of $4.8 \text{ mm} \times 4.8 \text{ mm}$. Distilled water droplet, which has the acoustic impedance of 1.5 MRayl, is more homogeneous shape on the right.